

# Acetylation of the CspA family protein CspC controls the type III secretion system through translational regulation of *exsA* in *Pseudomonas aeruginosa*

Shouyi Li, Yuding Weng, Xiaoxiao Li, Zhuo Yue, Zhouyi Chai, Xinxin Zhang, Xuetao Gong, Xiaolei Pan , Yongxin Jin, Fang Bai, Zhihui Cheng and Weihui Wu \*

State Key Laboratory of Medicinal Chemical Biology, Key Laboratory of Molecular Microbiology and Technology of the Ministry of Education, Department of Microbiology, College of Life Sciences, Nankai University, Tianjin 300071, China

Received February 27, 2021; Revised May 25, 2021; Editorial Decision May 27, 2021; Accepted June 08, 2021

## ABSTRACT

The ability to fine tune global gene expression in response to host environment is critical for the virulence of pathogenic bacteria. The host temperature is exploited by the bacteria as a cue for triggering virulence gene expression. However, little is known about the mechanism employed by *Pseudomonas aeruginosa* to respond to host body temperature. CspA family proteins are RNA chaperones that modulate gene expression. Here we explored the functions of *P. aeruginosa* CspA family proteins and found that CspC (PA0456) controls the bacterial virulence. Combining transcriptomic analyses, RNA-immunoprecipitation and high-throughput sequencing (RIP-Seq), we demonstrated that CspC represses the type III secretion system (T3SS) by binding to the 5' untranslated region of the mRNA of *exsA*, which encodes the T3SS master regulatory protein. We further demonstrated that acetylation at K41 of the CspC reduces its affinity to nucleic acids. Shifting the culture temperature from 25°C to 37°C or infection of mouse lung increased the CspC acetylation, which derepressed the expression of the T3SS genes, resulting in elevated virulence. Overall, our results identified the regulatory targets of CspC and revealed a regulatory mechanism of the T3SS in response to temperature shift and host *in vivo* environment.

## INTRODUCTION

Upon entering host, pathogenic bacteria encounter numerous challenges, including temperature shift, nutrient availability, antibacterial substances, immune cells, etc. The ability to fine tune gene expression in response to environmen-

tal changes is critical for bacterial survival and propagation. Temperatures around 37°C constitute a hallmark of mammal hosts, which serves as a key signal to turn on specific regulatory pathways to orchestrate bacterial virulence gene expression for successful colonization (1,2).

*Pseudomonas aeruginosa* is a wide-spread Gram-negative opportunistic pathogen of human that causes a variety of community-acquired and nosocomial infections in patients with burn wounds, cystic fibrosis and those with compromised immunity (3–5). A previous transcriptomic study revealed that close to 400 genes were alternatively expressed between 28°C and 37°C, indicating regulatory pathways responding to the temperature shift (6). Genes that were upregulated at 37°C include those related to the type III secretion system (T3SS) (6) that is a conserved virulence factor in Gram-negative pathogenic bacteria. The T3SS is a syringe-like apparatus that translocates effector proteins directly into the cytosols of a variety of eukaryotic cells, resulting in malfunction or death of the cells (7–9), which plays critical roles in the acute infections of *P. aeruginosa* (10–12).

Expression of the T3SS genes is highly energy consuming and thus is tightly controlled. ExsA is the master regulator that activates the expression of all the T3SS genes (13). The transcription of *exsA* is driven by two promoters — a promoter for the *exsC-exsE-exsB-exsA* operon ( $P_{exsC}$ ) and a promoter adjacent to the *exsA* coding region ( $P_{exsA}$ ). The  $P_{exsC}$  is directly regulated by ExsA (14–19), while the  $P_{exsA}$  is regulated by Vfr in conjunction with cAMP (20–23). The known T3SS inducing conditions include host cell contact, depletion of extracellular  $Ca^{2+}$  and serum albumin (24,25). The upregulation of the T3SS genes at 37°C indicates that the mammalian body temperature serves as one of the signals that coordinate expression of the T3SS genes in response to host environment. Elucidation of the temperature sensing and response pathways is critical to fully understand the bacterial virulence mechanisms.

\*To whom correspondence should be addressed. Tel: +86 22 23502210; Fax: +86 22 23502210; Email: wuweihui@nankai.edu.cn

**Disclaimer:** The funders had no role in study design, data collection and interpretation, or the decision to submit the work for publication.

CspA family proteins are a group of small nucleic acid binding proteins belonging to the cold shock domain protein family (26–28). These proteins share a conserved nucleic acid binding domain that is present in every kingdom of life (29–31). By binding to mRNAs, CspA family proteins controls various biological processes and bacterial response to environmental changes (32–39).

Here we show that a *P. aeruginosa* CspA family protein CspC controls the expression of T3SS genes by binding to the 5'UTR of the *exsA* mRNA. In addition, we demonstrate temperature responsive acetylation of CspC, which affects its nucleic acid binding ability and thus its regulatory effect on the *exsA*. In combination, our results reveal a global regulatory role of the CspC and a post-translational modification (PTM)-mediated bacterial response to mammalian *in vivo* environment.

## MATERIALS AND METHODS

### Bacterial strains and plasmids

Bacterial strains, plasmids and primers used in this study are listed in Supplementary Table S4. Both *P. aeruginosa* and *Escherichia coli* strains were cultured aerobically in LB medium (10 g/l tryptone, 5 g/l NaCl, 5 g/l yeast extract, pH 7.0–7.5). When needed, the medium for *P. aeruginosa* was supplemented with tetracycline (50 µg/ml) (BBI life sciences, Shanghai, China), gentamicin (50 µg/ml) (BBI life sciences) or carbenicillin (150 µg/ml) (BBI life sciences) and the medium for *E. coli* was supplemented with tetracycline (10 µg/ml), gentamicin (10 µg/ml) or ampicillin (100 µg/ml) (BBI life sciences).

### RNA isolation and quantitative RT-PCR (qRT-PCR)

Bacteria grown at indicated conditions were harvested by centrifugation at 12 000 g for 1 min and total RNA were isolated with an RNAprep pure bacteria kit (Tiangen Biotech, Beijing, China). cDNA was synthesized with a reverse transcriptase (TAKARA, Dalian, China). For quantitative reverse transcriptase-polymerase chain reaction (qRT-PCR), indicated specific primers were mixed with diluted cDNA and SYBR Premix Ex Taq II™ (TaKaRa). *rpsL* that encodes the 30 S ribosomal protein was used as an internal control. The results were determined and analyzed with the CFX Connect Real-Time system (Bio-Rad, USA).

### Mouse acute pneumonia model and histological procedures

All animal experiments were in accordance with Nankai University and Chinese national laboratory animal care and usage guidelines. The protocol was approved by the animal care and use committee of the College of Life Sciences, Nankai University and the permit number is NK-04-2012. To test the bacterial virulence, the indicated strains were cultured in LB to an OD<sub>600</sub> of 1.0, followed by centrifugation at 12 000 g for 1 min and the pellets were resuspended in phosphate-buffered saline (PBS) to 2 × 10<sup>8</sup> CFU/ml. 6-week-old female BALB/c mice (Vital River, Beijing, China) were anesthetized by intraperitoneal injection with 85 µl 7.5% chloral hydrate and then intranasally inoculated with ~4 × 10<sup>6</sup> CFU bacteria. Twelve hours post-infection (hpi),

mice were sacrificed with CO<sub>2</sub> and the lungs were removed. For bacterial colonization, the lungs were homogenized in 1% proteose peptone (Solarbio, Beijing, China) and bacterial loads were determined by plating. The hematoxylin and eosin (H&E) staining was performed as previously described (40). Briefly, the lungs were fixed with 4% paraformaldehyde (Servicebio, Wuhan, China) overnight, dehydrated in ethanol, embedded in paraffin, sectioned and stained with hematoxylin and eosin.

### Cell culture and lactate dehydrogenase (LDH) release assay

A549 cells were cultured with the Roswell Park Memorial Institute (RPMI) 1640 medium (Corning, USA) containing 10% fetal bovine serum (FBS) and 1% penicillin/streptomycin (Gibco, USA) at 37°C in 5% CO<sub>2</sub>. 2 × 10<sup>4</sup> cells were seeded into each well of a 96-well plate. The medium was replaced with antibiotic and FBS free RPMI 1640 3 h before bacterial infection. Bacteria were grown in LB at 37°C to an OD<sub>600</sub> of 1.0, and then washed twice and resuspended in PBS. A549 cells were infected with indicated *P. aeruginosa* strains at a multiplicity of infection (MOI) of 50. The plate was centrifuged at 1000 g for 5 min to synchronize the infection. Two hours post-infection, LDH present in the supernatant was measured by the LDH cytotoxicity assay kit (Beyotime, China). Cells treated with 1% Triton X-100 were used as the control of total release (100% LDH release) and the free RPMI 1640 medium was used as the negative control (0% LDH release). The cytotoxicity of bacteria was calculated following the manufacturer's instruction.

### β-galactosidase activity assay

The β-galactosidase activity assay was performed as previously described with minor modifications (41). Bacteria were grown in LB with or without 5 mM EGTA at 37°C until the OD<sub>600</sub> reached 1.0. The bacteria were collected and resuspended in 1 ml Z buffer (0.06 M Na<sub>2</sub>HPO<sub>4</sub>, 0.04 M NaH<sub>2</sub>PO<sub>4</sub>, 0.01 M KCl, 0.001 M MgSO<sub>4</sub> and 0.05 M β-mercaptoethanol). A total of 500 µl of the suspension was mixed with 10 µl 0.1% sodium dodecyl sulfate (SDS) and 10 µl chloroform by vortex. After the addition of 100 µl of 4 mg/ml orthonitrophenyl-galactopyranoside (ONPG) (BBI life sciences), the mixture was incubated at 37°C immediately. When the color turned light yellow, 500 µl 1M Na<sub>2</sub>CO<sub>3</sub> was added to stop the reaction. After recording the reaction time, OD<sub>600</sub> of the bacterial suspensions and OD<sub>420</sub> of the reaction mixtures were determined. The β-galactosidase activities (Miller units) were calculated as follows: Miller units = (1000 × OD<sub>420</sub>)/T/500/OD<sub>600</sub>; T, reaction time.

### RNA immunoprecipitation (RIP) and transcriptome sequencing analyses

Overnight culture of the Δ*cspC* mutant containing pMMB67EH-CspC-GST was subcultured in fresh LB containing 150 µg/ml carbenicillin at 37°C. 0.5 mM IPTG was added to the medium when the OD<sub>600</sub> reached 0.5. After 4 h induction at 37°C, the bacteria were harvested

by centrifugation and the CspC-GST recombinant protein was purified with a GST-tag Protein Purification Kit (Beyotime, China). A total of 1 mM DTT and RNase Inhibitor (Beyotime, China) was added to all liquid reagents in the process. The purified protein was mixed with three times the volume of TE buffer, followed by RNA isolation with an RNAPrep pure bacteria kit (Tiangen Biotech, Beijing, China).

The RNA-sequencing was performed by GENEWIZ (Suzhou, China). The RNA samples were quantified using a Qubit 2.0 Fluorometer (Invitrogen, Carlsbad, CA, USA) and qualified by Agilent Bioanalyzer 2100 (Agilent Technologies, Palo Alto, CA, USA) and NanoDrop (Thermo Fisher Scientific Inc.). A total of 1  $\mu$ g RNA and 10  $\mu$ g RNA immunoprecipitation (RIP) sample were used for the following library preparation.

Next generation sequencing library preparations were constructed according to the manufacturer's protocol (NEBNext<sup>®</sup> Ultra<sup>™</sup> Directional RNA Library Prep Kit for Illumina<sup>®</sup>). The rRNA was depleted from total RNA using Ribo-Zero rRNA Removal Kit (Bacteria) (Illumina). The ribosomal depleted mRNA was then fragmented and reverse transcribed. First strand cDNA was synthesized using ProtoScript II Reverse Transcriptase with random primers and Actinomycin D. The second strand cDNA was synthesized using Second Strand Synthesis Enzyme Mix (including dACGTP/dUTP). The double-stranded DNA was purified by AxyPrep Mag PCR Clean-up (Axygen) and then treated with End Prep Enzyme Mix to repair both ends and add a dA-tailing in one reaction, followed by a T-A ligation to add adaptors to both ends. Size selection of the adaptor-ligated DNA was then performed using AxyPrep Mag PCR Clean-up (Axygen), and fragments of  $\sim$ 360 bp (with the approximate insert size of 300 bp) were recovered. The dUTP-marked second strand was digested with the Uracil-Specific Excision Reagent (USER) enzyme (New England Biolabs). Each sample was then amplified by PCR for 11 cycles using P5 and P7 primers as instructed by the Manual of NEBNext<sup>®</sup> Ultra<sup>™</sup> II Directional RNA Library Prep Kit for Illumina<sup>®</sup> (New England Biolabs). Both the P5 and P7 primers carry sequences that can anneal with flow cell to perform bridge PCR and P7 primer carrying a six-base index allowing for multiplexing. The PCR products were cleaned up using the AxyPrep Mag PCR Clean-up (Axygen), validated using an Agilent 2100 Bioanalyzer (Agilent Technologies, Palo Alto, CA, USA) and quantified by Qubit 2.0 Fluorometer (Invitrogen, Carlsbad, CA, USA).

Then libraries with different indices were multiplexed and loaded on an Illumina HiSeq instrument according to manufacturer's instructions (Illumina, San Diego, CA, USA). Sequencing was carried out using a 2  $\times$  150 paired-end (PE) configuration, sequence reads analysis was based on the predicted genes of strain PA14 (<http://www.pseudomonas.com>) (42). Differential expression analysis used the DESeq Bioconductor package, a model based on the negative binomial distribution. The sequencing was performed with each single sample of the wild-type PA14 and the  $\Delta$ cspC mutant. After adjusted by Benjamini and Hochberg's approach for controlling the false discovery rate, *P*-value of genes were setted  $<0.05$  to detect differential expressed ones. The en-

tire transcriptome sequencing data have been submitted in the NCBI SRA, with accession number PRJNA690968.

### Electrophoretic mobility shift assay

Both dsDNA and ssDNA fragments corresponding to the sequences upstream of the *exsA* coding region were synthesized by GENEWIZ. A total of 40 ng DNA were incubated with 0 to 2 mM purified GST-CspC protein at 16 or 25°C for 30 min in a 20  $\mu$ l reaction (10 mM Tris-HCl, pH 7.6, 4% glycerol, 1 mM ethylenediaminetetraacetic acid, 5 mM CaCl<sub>2</sub>, 100 mM NaCl). The samples were loaded onto an 8% native polyacrylamide gel that had been pre-run for over 1 h. The electrophoresis was performed on ice at 120 V for 1 h or 1.5 h. The gel was stained with 0.5  $\times$  TBE containing SYBR<sup>®</sup> Gold nucleic acid gel stain for ssDNA and 0.5  $\times$  TBE containing 0.5  $\mu$ g/ml ethidium bromide for dsDNA. Bands were visualized with a molecular imager ChemiDoc<sup>™</sup> XRS+ (Bio-Rad).

### Western blot

Protein samples from equivalent amounts of bacterial culture were loaded onto a 12% SDS-polyacrylamide gel electrophoresis (SDS-PAGE) gel. Proteins were transferred to a polyvinylidene difluoride (PVDF) membrane (Millipore, USA). The membrane was incubated with a mouse monoclonal anti-His antibody (CST, USA), a rabbit monoclonal anti-Flag antibody (Sigma, USA), a rabbit monoclonal anti-Glutathione-S-Transferase (GST) antibody (Sigma, USA) or a mouse monoclonal anti-RNA polymerase  $\alpha$  antibody (Biolegend). For determination of acetylation, equivalent amounts of purified proteins were loaded onto a 12% SDS-PAGE gel, and then transferred to a PVDF membrane. The membrane was incubated with a rabbit monoclonal anti-GST antibody (Sigma, USA) or a mouse monoclonal anti-acetyllysine antibody (Jingjie PTM Biolab, China). Signals were detected with an Immobilon<sup>™</sup> Western kit (Millipore).

### RNA extraction and protein purification from *in vivo* samples

RNA extraction from *in vivo* samples was performed as previously described with minor modification (43). Briefly, BALB/c mice were intranasally inoculated with 4  $\times$  10<sup>7</sup> CFU of indicated strains and sacrificed 6 hpi. The bronchoalveolar lavage fluid (BALF) was collected as previously described (44). A total of 20  $\mu$ l of the BALF was used for bacterial counting. The remaining BALF was centrifuged and the pellets were resuspended in 200  $\mu$ l TRIzol reagent (Thermo Fisher Scientific, USA), followed by RNA purification as instructed by the manufacturer.

To purify the CspC-GST fusion protein, we used a PA14  $\Delta$ pseC mutant containing the *cspC-gst* fusion driven by the native *cspC* promoter on pUCP20. Each mouse was infected with 1  $\times$  10<sup>9</sup> CFU of the bacteria. At 4 hpi, BALF was collected and the bacteria were harvested by centrifugation. Then the pellets from 20 mice were mixed, followed by purification of the CspC-GST protein with a GST-tag Protein Purification Kit (Beyotime, China).

## LC-MS/MS analysis

The LC-MS/MS analysis was performed by the PTM Biolab (Hangzhou, China). The tryptic peptides were dissolved in 0.1% formic acid (solvent A), directly loaded onto a home-made reversed-phase analytical column (15-cm length, 75  $\mu\text{m}$  i.d.). The gradient was comprised of an increase from 6 to 23% solvent B (0.1% formic acid in 98% acetonitrile) over 16 min, 23 to 35% in 8 min and climbing to 80% in 3 min then holding at 80% for the last 3 min, all at a constant flow rate of 400 nl/min on an EASY-nLC 1000 UPLC system.

The peptides were subjected to NSI source followed by tandem mass spectrometry (MS/MS) in Q Exactive™ Plus (Thermo) coupled online to the UPLC. The electrospray voltage applied was 2.0 kV. The m/z scan range was 350–1800 for full scan, and intact peptides were detected in the Orbitrap at a resolution of 70 000. Peptides were then selected for MS/MS using NCE setting as 28 and the fragments were detected in the Orbitrap at a resolution of 17 500. A data-dependent procedure that alternated between one MS scan followed by 20 MS/MS scans with 15.0 s dynamic exclusion. Automatic gain control was set at 5E4.

## mRNA stability assay

The mRNA stability assay was performed as previously described (41). Wild-type PA14 and the  $\Delta\text{cspC}$  mutant were grown in LB at 37°C to an OD<sub>600</sub> of 1.0, followed by treatment with 500  $\mu\text{g/ml}$  rifampin. At indicated time points, equivalent numbers of bacterial cells were collected. Each sample was mixed with equal number of *E. coli* cells expressing the *gfp* gene. Total RNA was extracted, and the *rpsL* and the *exsA* mRNA levels in each sample were determined by real-time PCR using *gfp* as the internal control.

## RESULTS

### Expression patterns of CspA family proteins in *P. aeruginosa*

The *P. aeruginosa* wild-type strain PA14 harbors five *cspA* homologous genes, namely PA0456, PA0961, PA1159, PA2622 (*cspD*) and PA3266 (*capB*) (45). All of the five encode proteins contain a highly conserved oligonucleotide binding (OB)-fold motif (46) (Supplementary Figure S1a). The evolutionary relationships between the CspA family proteins in *P. aeruginosa* and *E. coli* were evaluated by constructing a neighbor-joining phylogenetic tree using MEGA X (47) (Supplementary Figure S1b). To examine whether the expression of these genes responds to temperature shift, we cultured wild-type PA14 at 37°C to an OD<sub>600</sub> of 0.5, followed by shifting to 16°C. After 1 h culture, half of the cells was switched back to 37°C, while the other half was remained at 16°C. At indicated time points along the experiment, the bacterial cells were collected and the mRNA levels of the five *csp* genes were determined by qRT-PCR (Supplementary Figure S2a). As shown in Supplementary Figure S2b, all of the cold shock genes were upregulated after growth at 16°C for 1 or 4 h. When the culture temperature was shifted back to 37°C, the expression of PA0456, PA0961 and *capB* was downregulated, whereas the mRNA levels of PA1159 and *cspD* kept increasing (Supplementary Figure S2b). Previous studies in *E. coli* demonstrated

that the expression of CspA family proteins could be influenced by growth phases (48,49). In the *P. aeruginosa* strain PA14, our experimental results revealed that the expression of PA1159, *capB* and *cspD* was increased in the stationary phase (Supplementary Figure S2c). Thus, PA1159 and *cspD* might be regulated in response to both temperature and growth phase. In our experiment, the bacterial OD<sub>600</sub> reached 1.8 after switching from 16°C to 37°C and grown for 1 h, which might result in the increased mRNA levels of the PA1159 and *cspD*. In combination, all the five CspA homologs in *P. aeruginosa* are regulated in response to temperature shift, and the expression of PA1159, *capB* and *cspD* is also influenced by growth phases.

### PA0456 influences the bacterial virulence in a mouse acute pneumonia model

To test whether the five CspA homologs are involved in the virulence of *P. aeruginosa*, we constructed in-frame deletion mutants of each of the *cspA* family genes in PA14 and examined the bacterial virulence in a mouse acute pneumonia model. Mutation of PA0456, but not the other four genes, increased the bacterial loads in the lungs (Figure 1A and Supplementary Figure S3a). To examine whether the enhanced virulence of the  $\Delta\text{PA0456}$  mutant is due to increased growth rate, we monitored the bacterial growth *in vitro*. In LB medium, the  $\Delta\text{PA0456}$  mutant grew at the same rate as the wild-type PA14 (Supplementary Figure S3b). These results revealed a role of the PA0456 in modulating the bacterial virulence. Sequence analysis revealed that PA0456 is highly homologous to the *E. coli* CspC and CspE (Supplementary Figure S1b and Table.S1). Complementation with the *E. coli cspC* or *cspE* gene restored the mRNA levels of *exsA* and *exsC* in the  $\Delta\text{PA0456}$  mutant (Supplementary Figure S4), indicating a functional similarity between PA0456 and the *E. coli cspC* or *cspE*. Since PA0456 is slightly more similar to the *E. coli* CspC, we designated PA0456 as CspC and conducted further functional studies.

### CspC represses the expression of T3SS genes

To understand the mechanism of CspC-mediated regulation on the bacterial virulence, we performed transcriptome sequencing analyses and found that 174 genes were differentially expressed in the  $\Delta\text{cspC}$  mutant (Supplementary Table S2). Of note, all the T3SS genes were upregulated in the  $\Delta\text{cspC}$  mutant (Figure 1B). qRT-PCR results verified that deletion of the *cspC* resulted in higher mRNA levels of *exsA*, *exsC* and *pcrV* under both T3SS non-inducing and inducing conditions, which were restored by complementation with an intact *cspC* gene (Figure 1C). By utilizing a plasmid encoding a 6  $\times$  His-tagged *exoU* driven by its native promoter, we observed that the ExoU-His protein level was also increased in the *cspC* mutant strain (Figure 1D).

Since the T3SS plays a major role in the bacterial cytotoxicity, we performed a lactate dehydrogenase (LDH) release assay with the human lung epithelial cell A549. As shown in Figure 1E, the cytotoxicity of the  $\Delta\text{cspC}$  mutant was higher than the wild-type PA14 and the complemented strain. In combination, these results demonstrate a negative regulatory role of the CspC on the T3SS genes.

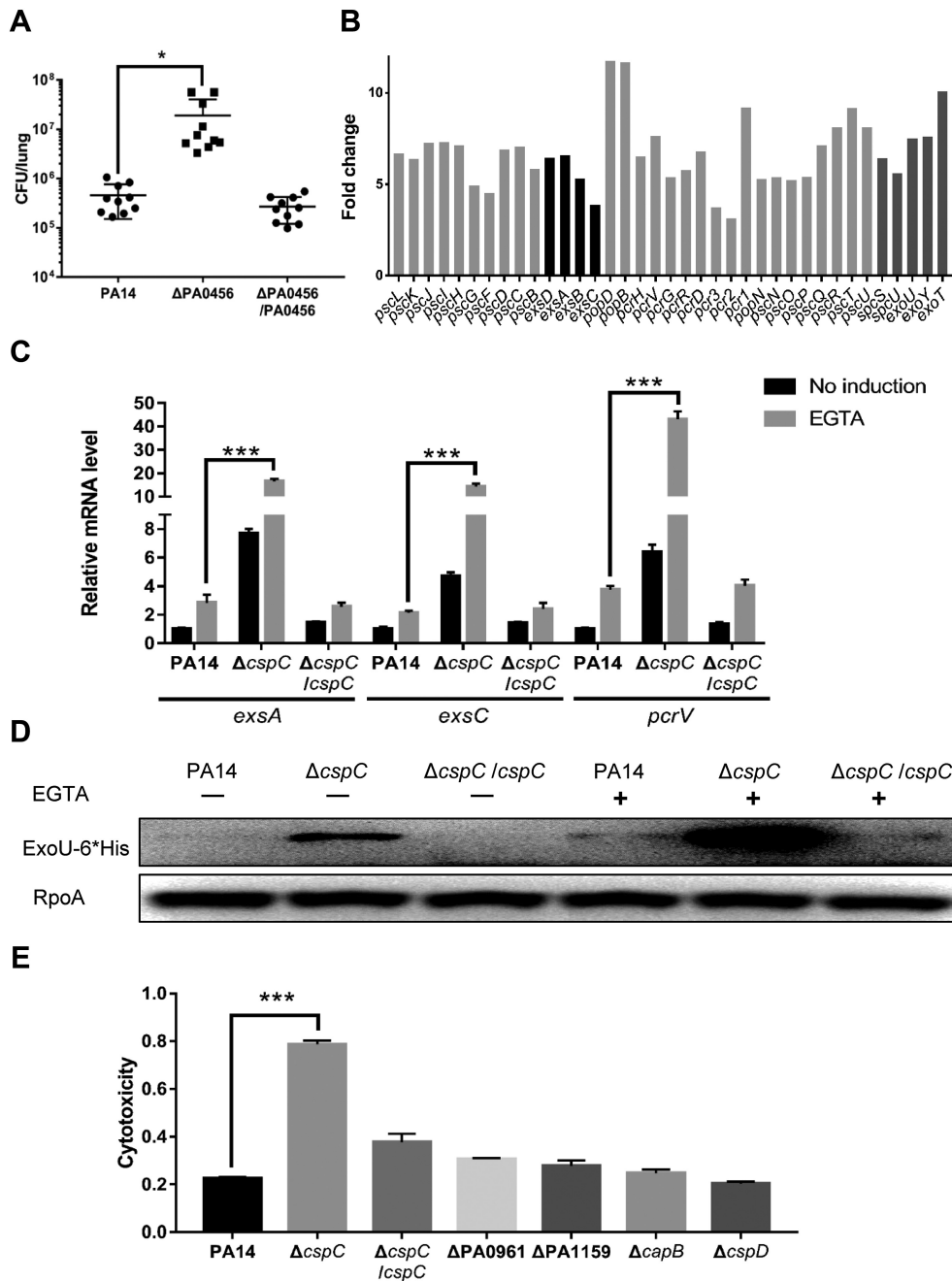


**Figure 1.** Mutation of PA0456 increases the bacterial virulence in a mouse acute pneumonia model. (A) Mice were inoculated intranasally with  $4 \times 10^6$  CFU of the indicated strains. At 12 hpi, the mice were sacrificed and lungs were isolated and homogenized. The bacterial loads were determined by serial dilution and plating. The central bar indicates the mean, and the error bar indicates standard error.  $*P < 0.05$  by the Mann–Whitney test. (B) Fold changes of the mRNA levels of the T3SS genes in the  $\Delta cspC$  mutant. The wild-type PA14 and the  $\Delta cspC$  mutant were grown to an OD<sub>600</sub> of 1.0 in LB at 37°C, followed by RNA isolation and RNA-seq analyses. The dark gray, gray and black bars represent the effector, structural and regulatory genes of the T3SS, respectively. (C) Total RNA was isolated from bacteria grown in LB with or without 5 mM EGTA at 37°C and the relative mRNA levels of *exsA*, *exsC*, *pcrV* were determined by qRT-PCR. Data represent the mean of three independent experiments and error bars indicate standard deviation.  $***, P < 0.001$  by Student's *t*-test. (D) Bacteria carrying an *exoU-6* × His driven by its native promoter ( $P_{exoU-exoU-6}$  × His) were grown to an OD<sub>600</sub> of 1.0 in LB containing 150 μg/ml carbenicillin with or without 5 mM EGTA. The ExoU-6 × His levels were determined by western blot. (E) A549 cells were infected with the indicated strains at a MOI of 50 for 3 h. The bacterial cytotoxicity was determined by the LDH release assay. The data shown represent the results from three independent experiments.  $***, P < 0.001$  by Student's *t*-test.

### The regulatory role of CspC on the promoters of *exsC* and *exsA*

Since the mRNA level of the T3SS master regulator gene *exsA* was increased in the  $\Delta cspC$  mutant, we explored the mechanism of CspC-mediated regulation on *exsA*. The *exsA* gene is driven by  $P_{exsA}$  and  $P_{exsC}$  (Figure 2A) that are directly controlled by Vfr/cAMP and ExsA, respectively (23). Thus, the expression of *exsA* is regulated through an autoactivation loop (Figure 2A). To examine whether CspC affects the transcription of *exsA*, we constructed three  $\beta$ -galactosidase transcriptional fusions, namely  $P_{exsC}$ -*lacZ*,  $P_{exsC-A}$ -*lacZ* and  $P_{exsA}$ -*lacZ* (Figure 2A). The expression levels of  $\beta$ -galactosidase from the  $P_{exsC}$ -*lacZ* and  $P_{exsC-A}$ -*lacZ* were increased in the  $\Delta cspC$  mutant in the presence or absence of EGTA, indicating an elevated activity of the *exsC* promoter ( $P_{exsC}$ ). However, the expression levels of  $\beta$ -galactosidase from the  $P_{exsA}$ -*lacZ* were similar in wild-type PA14 and the  $\Delta cspC$  mutant (Figure 2B). To further verify the role of CspC on the  $P_{exsA}$  activity, we inserted two tandem transcription terminators (T0T1) between the *exsB* coding region and the  $P_{exsA}$  (Figure 2A), which blocks the read-through transcription from *exsC* to *exsA*, leaving the transcription of *exsA* solely dependent on the  $P_{exsA}$ . Insertion of the T0T1 in the chromosome of PA14 or the  $\Delta cspC$  mutant resulted in similar *exsA* and *exsC* mRNA levels in the presence or absence of EGTA (Figure 2C). In combination, these results demonstrate that CspC controls the T3SS by influencing the activity of the *exsC* promoter but not the *exsA* promoter.

### Identification of the CspC regulatory targets by RIP-seq

To understand the mechanism of CspC-mediated regulation of the T3SS, we overexpressed a C-terminus GST-tagged CspC (CspC-GST) or a GST protein alone in wild-type PA14 and performed RIP-seq analyses. Total bacterial RNA was quantified by RNA-seq and used as the input. Our results demonstrated that CspC represses the T3SS genes under non-inducing condition (without EGTA) (Figure 1C and D), indicating that CspC binds to its targets under this condition. Meanwhile, addition of EGTA retarded the bacterial growth (data not shown), which might interfere with the expression of the *cspC*-GST driven by the exogenous *tac* promoter. Thus, we performed the RIP and RNA-seq assays under the T3SS non-inducing condition. The CspC-GST or GST was purified through affinity chromatography under a native condition, followed by RNA extraction. The amount of RNA from the GST RIP sample was too low to perform RNA-seq. Thus, only the CspC-GST RIP sample was subjected to RNA-seq. The relative enrichment fold was calculated as number of reads in the RIP-seq (output) divided by the number of reads of the corresponding RNA fragment in the RNA-seq (input). The enriched RNA fragments were shown in Figure 3A and listed in Supplementary Table S3. Of note, a fragment containing the *exsA* mRNA and its 5'UTR was enriched 3.63 folds by the CspC-GST (Figure 3A and B). A RIP-coupled qRT-PCR assay confirmed the enrichment of the fragment (Figure 3C). These results indicate a possible post-transcriptional regulation of the *exsA* mRNA by CspC.

### CspC controls the expression of *exsA* at the post-transcriptional level

To examine whether CspC controls *exsA* at the post-transcriptional level, we constructed a C-terminus FLAG-tagged *exsA* driven by an exogenous  $P_{tac}$  promoter. Based on the RIP-seq result, a 120 bp fragment upstream of the *exsA* coding region was included in the construct, resulting in  $P_{tac}$ -120-*exsA*-FLAG (Figure 3D). The ExsA-FLAG level was higher in the  $\Delta cspC$  mutant under both T3SS inducing and non-inducing conditions (Figure 3E). To narrow down the region that is involved in the post-transcriptional regulation, we reduced the 5'UTR to 74 bp (designated as  $P_{tac}$ -74-*exsA*-FLAG), which displayed the similar expression pattern as the  $P_{tac}$ -120-*exsA*-FLAG (Figure 3E). However, reduction of the 5' UTR to 25 bp ( $P_{tac}$ -25-*exsA*-FLAG) resulted in similar expression levels of ExsA-FLAG in wild-type PA14 and the  $\Delta cspC$  mutant (Figure 3E). To examine whether the *exsA* coding region is involved in the post-transcriptional regulation, we fused the 74 bp 5'UTR to a *gst* gene, resulting in  $P_{tac}$ -74-*gst* (Figure 3F). The GST level was higher in the  $\Delta cspC$  mutant than that in the wild-type PA14 (Figure 3G), indicating a critical role of the 74 bp sequence in the CspC-mediated post-transcriptional regulation.

We then performed electrophoretic mobility shift assays (EMSA) to confirm the binding between CspC and the 5'UTR fragment. Previous studies demonstrated that CSPs binds to ssDNA as efficiently as RNA (38,50). Therefore, we used ssDNAs in the EMSAs. As shown in Figure 3H, CspC retarded the motility of the 74 nt ssDNA that represents the *exsA* 5'UTR. However, no obvious retardation was observed with the complementary ssDNA (Figure 3H), a 143 bp dsDNA of the 5' UTR sequence of *exsA* or a 74 nt ssDNA of the *cspC* coding region (Supplementary Figure S5a and b). In addition, the *exsA* mRNA stability in the  $\Delta cspC$  mutant was similar as that in the wild-type PA14 (Supplementary Figure S5c and d). Taken together, these results demonstrate that CspC controls the translation of the *exsA* mRNA through its 74 nt 5'UTR.

A previous study demonstrated that the RNA helicase DeaD controls the translation of the *exsA* mRNA through the 37 bp 5'UTR and the coding region (51). We thus examined whether CspC interplays with DeaD in the post-transcriptional regulation of *exsA*. Deletion of the *deaD* gene reduced the expression level of the ExsA-FLAG from the  $P_{tac}$ -74-*exsA*-FLAG (Supplementary Figure S6a). However, dual deletion of *cspC* and *deaD* ( $\Delta cspC\Delta deaD$ ) resulted in a similar level of the 74-ExsA-FLAG as that in the wild-type PA14 (Supplementary Figure S6a). We then constructed a FLAG-tagged *exsA* gene with the 37 bp native *exsA* 5'UTR driven by the  $P_{tac}$  promoter, resulting in  $P_{tac}$ -37-*exsA*-FLAG. Consistent with the previous report, deletion of the *deaD* gene reduced the expression level of the 37-ExsA-FLAG (Supplementary Figure S6b). However, the 37-ExsA-FLAG levels in the  $\Delta cspC$  and  $\Delta cspC\Delta deaD$  mutants were similar as those in the wild-type PA14 and the  $\Delta deaD$  mutant, respectively (Supplementary Figure S6b). Meanwhile, expression of the 74-GST from the  $P_{tac}$ -74-*gst* was not affected by the deletion of *deaD* (Supplementary Figure S6c), thus verifying the involvement of the *exsA* coding region in the DeaD-mediated translational regulation.

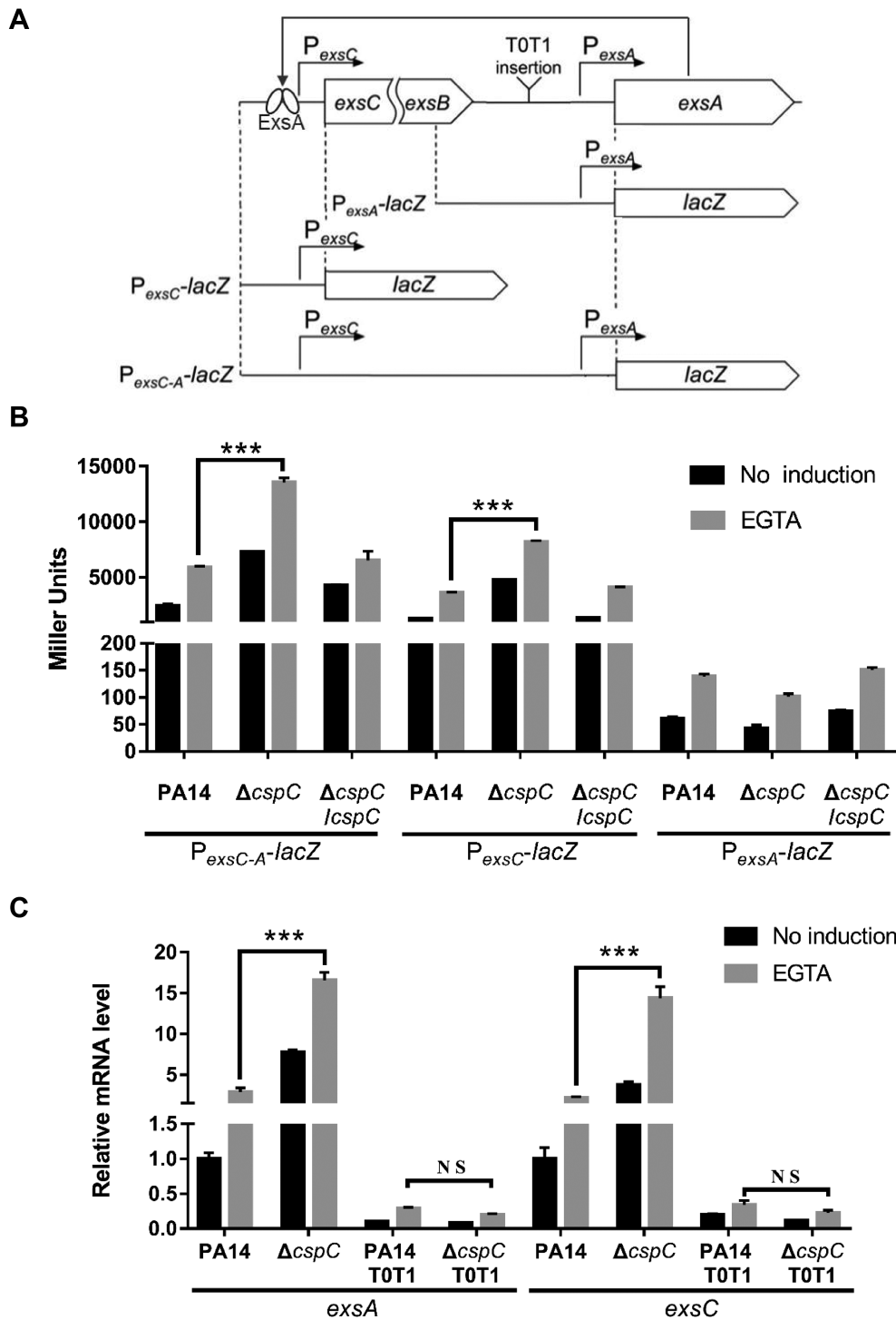


**Figure 2.** The roles of CspC in the regulation of the promoters of *exsC* and *exsA*. (A) Schematic diagram of the *exsCEBA* operon and the  $P_{exsC}$ -*lacZ*,  $P_{exsA}$ -*lacZ* and  $P_{exsC-A}$ -*lacZ* transcriptional fusions. The  $P_{exsC}$  and  $P_{exsA}$  were indicated by arrows. ExsA binds to the promoter region of the *exsCEBA* operon and activates its expression. The insertion site of the transcriptional terminators T0T1 was indicated. (B) Bacteria carrying the  $P_{exsC}$ -*lacZ*,  $P_{exsA}$ -*lacZ* and  $P_{exsC-A}$ -*lacZ* were grown at 37°C in LB containing 50 µg/ml tetracycline with or without 5 mM EGTA. The Miller units were the means of results of at least three independent experiments. \*\*\*,  $P < 0.001$  by Student's *t*-test. (C) The bacteria were grown at 37°C in LB with or without 5 mM EGTA and the mRNA levels of *exsA* and *exsC* were determined by quantitative real-time PCR. Data represent the mean of three independent experiments and error bars indicate standard deviation. \*\*\*,  $P < 0.001$ ; NS, not significant by Student's *t*-test.

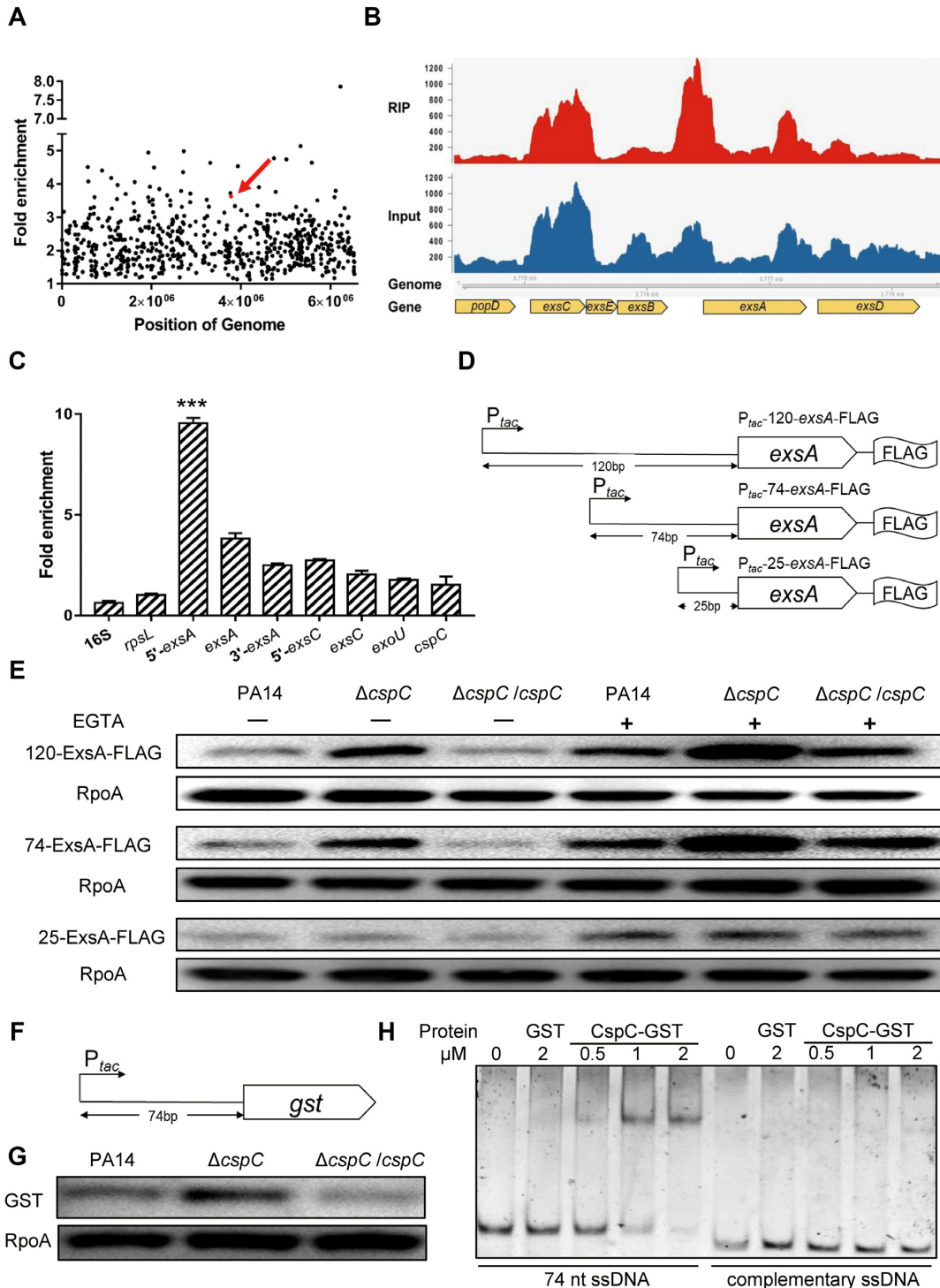


**Figure 3.** CspC controls the expression of *exsA* at the post-transcriptional level. (A) Enriched RNA fragments by RIP-seq. Each dot indicates an enriched RNA fragment. The fragment containing the *exsA* mRNA and its 5'UTR was shown as a red dot and indicated by a red arrow. (B) Standardized reads distributions of the peak regions of the RIP-seq and RNA-seq (input) results. The open reading frames on the chromosome are indicated in the lowest panel. (C) Fold enrichment of the indicated fragments tested by an RIP-coupled qRT-PCR assay. Data represent the mean of three independent experiments and error bars indicate standard deviation. \*\*\*,  $P < 0.001$  compared to the other samples by Student's *t*-test. (D) Schematic diagram of the *exsA*-FLAG fusions driven by a *tac* promoter with indicated length of upstream regions. (E) Bacteria carrying the *exsA*-FLAG with indicated upstream segments ( $P_{tac}$ -120/74/25-*exsA*-FLAG) were grown to an  $OD_{600}$  of 1.0 at 37°C in LB containing 150 µg/ml carbenicillin with or without 5 mM EGTA. The ExsA-FLAG levels were determined by western blot. (F) Schematic diagram of a *gst* gene driven by a *tac* promoter with the 74 bp upstream region of *exsA* ( $P_{tac}$ -74-*gst*). (G) Indicated strains carrying the  $P_{tac}$ -74-*gst* were grown to an  $OD_{600}$  of 1.0 at 37°C in LB containing 150 µg/ml carbenicillin. The amounts of GST and RpoA were determined by western blot. (H) The purified CspC-GST was incubated with a 74 nt ssDNA that represents the 74 nt 5'-UTR of the *exsA* mRNA and a complementary ssDNA for 30 min at 16°C. The samples were subjected to electrophoresis in a native gel, followed by staining with SYBR Gold Nucleic Acid Gel Stain.

In the  $\Delta cspC\Delta deaD$  mutant, the 74-GST level was similar as that in the  $\Delta cspC$  mutant (Supplementary Figure S6c). In combination, these results indicate that DeaD and CspC regulate the translation of *exsA* independently.

### The CspC is acetylated in a temperature-dependent manner

Next, we explored the CspC-mediated signaling pathway that controls the T3SS. A previous study demonstrated upregulation of the T3SS genes when the culture temperature was shifted from 28°C to 37°C (6). By growth of the wild-type PA14 at room temperature (25°C) and 37°C, we did confirm the upregulation of the T3SS genes at 37°C (Figure 4B). Utilizing the  $P_{tac}$ -74-*exsA*-FLAG, we found that the ExsA-FLAG level was 2.95-fold higher at 37°C than that at 25°C in the wild-type PA14 (Figure 4A). In the  $\Delta cspC$  mutant, the ExsA-FLAG levels were 4.6- and 1.9-fold higher than those in the wild-type PA14 at 25°C and 37°C, respectively (Figure 4A), indicating that CspC represses the translation of *exsA* to a greater extent at 25°C.

We then compared the expression levels of CspC at 25°C and 37°C. The mRNA and protein levels of CspC were similar at the two temperatures (Figure 4B and C), which intrigued us to speculate a PTM of the CspC. An LC-MS/MS analysis of the CspC-GST purified from the  $\Delta cspC$  mutant grown at 37°C revealed an acetylation at position K41 (Figure 4E). In addition, higher amount of acetylated CspC-GST was observed from cells grown at 37°C than that at 25°C (Figure 4D). As a control, no acetylation was found on the GST protein (Supplementary Figure S7).

To examine whether the K41 acetylation affects the CspC function, we constructed K41Q and K41R mutant versions of the *cspC*, which mimic the acetylated and unacetylated states, respectively (52). EMSA results demonstrated that the K41Q mutation reduced the binding between CspC and the 74 nt ssDNA (Figure 5A). A surface plasmon resonance (SPR) assay revealed that the affinity of K41R CspC to the 74 nt ssDNA was ~10-fold higher than that of K41Q CspC (Figure 5B).

Overexpression of the K41R *cspC* in the  $\Delta cspC$  mutant reduced the mRNA levels of *exsA*, *exsC* and *pcrV*, whereas overexpression of the K41Q *cspC* did not affect the expression of the three genes (Figure 5C). As a control, overexpression of *cspC* variants with mutations at an unacetylated K48 residue (K48Q, K48R) in the  $\Delta cspC$  mutant resulted in similar effects as expressing the wild-type *cspC* (Figure 5C). We then examined the effects of the *cspC* mutants on the translation of *exsA* using the  $P_{tac}$ -74-*exsA*-FLAG. Compared to the wild-type *cspC*, the K41Q mutation is abolished of its repressor function on the translation of the *exsA*-FLAG (Figure 5D). Overexpression of the K41R *cspC* in the  $\Delta cspC$  mutant repressed the production of the ExsA-FLAG and resulted in similar levels of the ExsA-FLAG at 25°C and 37°C (Figure 5D), demonstrating a constitutive repression on the translation of *exsA*. However, the ExsA-FLAG level in the K41R *cspC* overexpressing strain was higher than that of overexpressing the wild-type *cspC* at 25°C (Figure 5D), which might be due to the aberrant folding of the K41R CspC protein. Nevertheless,

our results suggest that acetylation at the K41 residue modulates the function of CspC.

### Acetylation of the CspC at K41 modulates the expression of T3SS genes and the bacterial virulence *in vivo*

To examine whether CspC is acetylated *in vivo*, we infected mice intranasally with a  $\Delta pscC$  mutant carrying the *cspC*-*gst* driven by the *cspC* native promoter. The *pscC* gene encodes a structural component of the T3SS machinery (53,54), mutation of which attenuates the bacterial virulence, thus allowing a high infection dose for the isolation of the CspC-GST. Compared to the CspC-GST isolated from cells grown in LB at 25°C and 37°C, a higher level of acetylation was observed on the protein isolated from BALF of the infected mice. We then infected mice with the wild-type PA14, the  $\Delta cspC$  mutant carrying the *cspC* or the K41R, K41Q variant of *cspC*. Infection with the  $\Delta cspC$  mutant expressing *cspC*(K41R) resulted in reduced bacterial load and host inflammatory response compared to those by the  $\Delta cspC$  mutant (Figure 6A–C). However, the *cspC*(K41Q) did not affect the bacterial load of the  $\Delta cspC$  mutant or the host inflammatory response (Figure 6B and C). In addition, complementation with the *cspC*(K41R), but not the *cspC*(K41Q), in the  $\Delta cspC$  mutant reduced the mRNA levels of *exsA*, *exsC* and *pcrV* *in vitro* as well as *in vivo* (Figure 6D). In combination, these results indicate that the *in vivo* activity of the CspC is influenced by the acetylation of the K41.

## DISCUSSION

In this study, we examined the expression patterns of the five CspA family proteins in *P. aeruginosa* and studied their roles in bacterial virulence. Switching the culture temperature from 37°C to 16°C resulted in up regulation of all the CspA family protein genes, suggesting physiological roles of the CspA family proteins in response to cold shock.

In the acute pneumonia model, mutation of the *cspC* resulted in higher bacterial load and elevated inflammation. Transcriptome analyses revealed up regulation of the T3SS in the  $\Delta cspC$  mutant. Combining RIP-Seq and translational fusion assays, we show that CspC represses the translation of the *exsA* mRNA by binding to the 74 nt fragment of its 5'-UTR. The CspC and CspE in *Salmonella typhimurium* play important roles in the bacterial virulence (55). A previous study in *Staphylococcus aureus* revealed a role of CspA in the regulation of proteins involved in metabolism, bacterial aggregation, response to oxidative stress and virulence (38). Further studies revealed that the CspA binds to the U-rich region of the 5'-UTR of its mRNA, which melts the stem-loop of the RNA and blocks the processing of RNase III, resulting in repression of its own mRNA translation (38). CspA family proteins have also been found to function as anti-terminators of transcription by altering the mRNA secondary structure, which allows the transcription of downstream genes under low temperatures in various bacteria, such as *E. coli* and *Bacillus subtilis* (34). We speculate that the binding of CspC to the 5'-UTR of the *exsA* mRNA might alter the RNA sec-

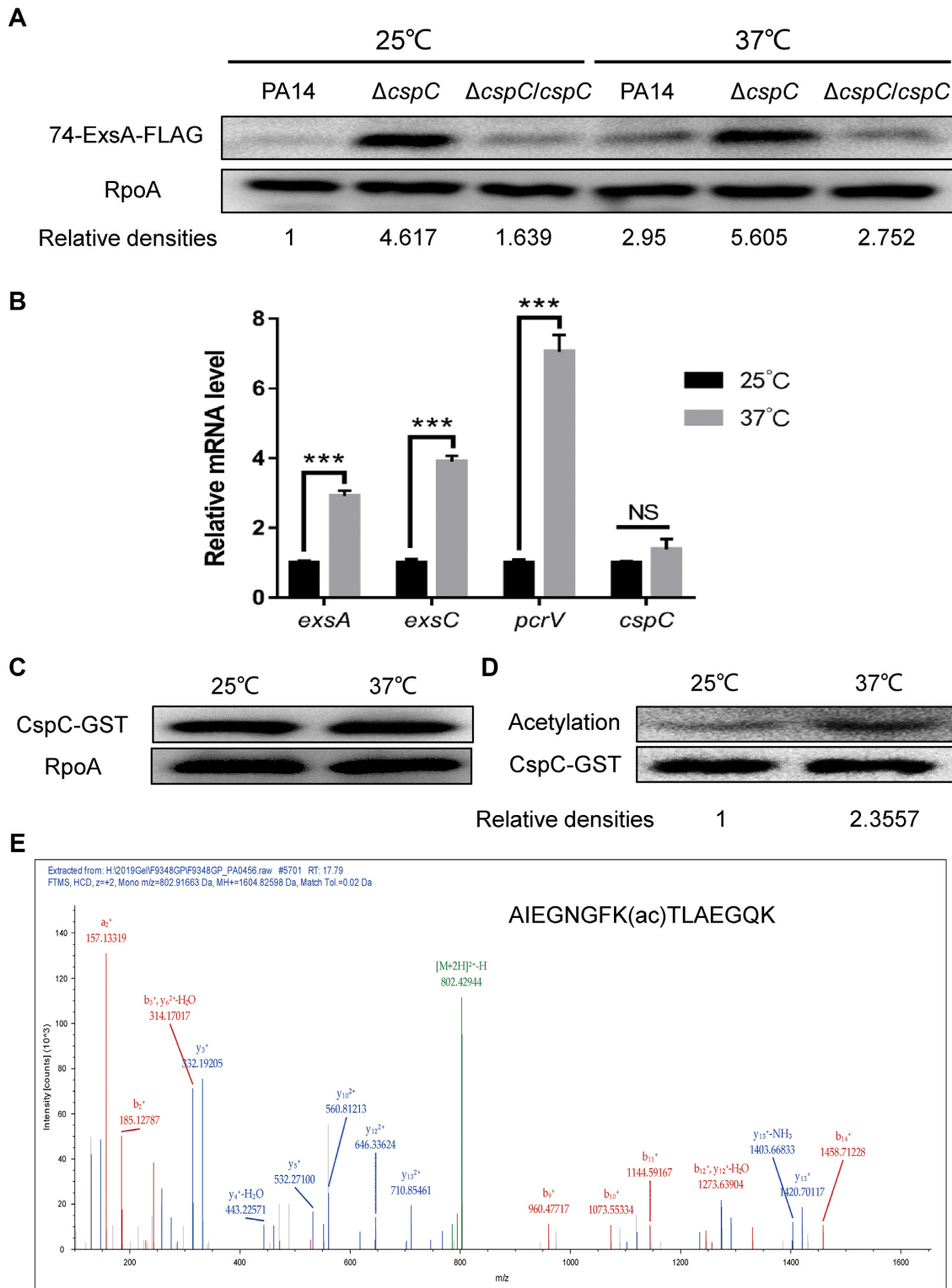


**Figure 4.** The activity of CspC is regulated by acetylation. **(A)** Indicated strains carrying the  $P_{lac}$ -74-*exsA*-FLAG were grown to an  $OD_{600}$  of 1.0 in LB containing 150  $\mu$ g/ml carbenicillin at 25°C or 37°C. The ExsA-FLAG levels were determined by western blot. **(B)** Relative mRNA levels of *exsA* and *cspC*. Total RNA of the wild-type PA14 was isolated from bacteria grown at 25°C or 37°C and mRNA levels of *exsA* and *cspC* were determined by qRT-PCR. Data represent the mean of three independent experiments and error bars indicate standard deviation. \*\*\*,  $P < 0.001$ , NS, not significant by Student's *t*-test. **(C)** Wild-type PA14 carrying a *cspC*-GST driven by its own promoter were grown to an  $OD_{600}$  of 1.0 in LB containing 150  $\mu$ g/ml carbenicillin under 25°C or 37°C. The amounts of GST and RpoA were determined by western blot. **(D)** Acetylation levels of the CspC-GST protein under 25°C or 37°C. Acetylation and the total amounts of the purified CspC-GST were determined by western blot. **(E)** MS/MS spectra of the acetylated lysine peptide. The CspC-GST was purified from the  $\Delta cspC$  mutant and subjected to the LC-MS/MS analysis. The b ion refers to the N-terminal parts of the peptide, and the y ion refers to the C-terminal parts of the peptide.

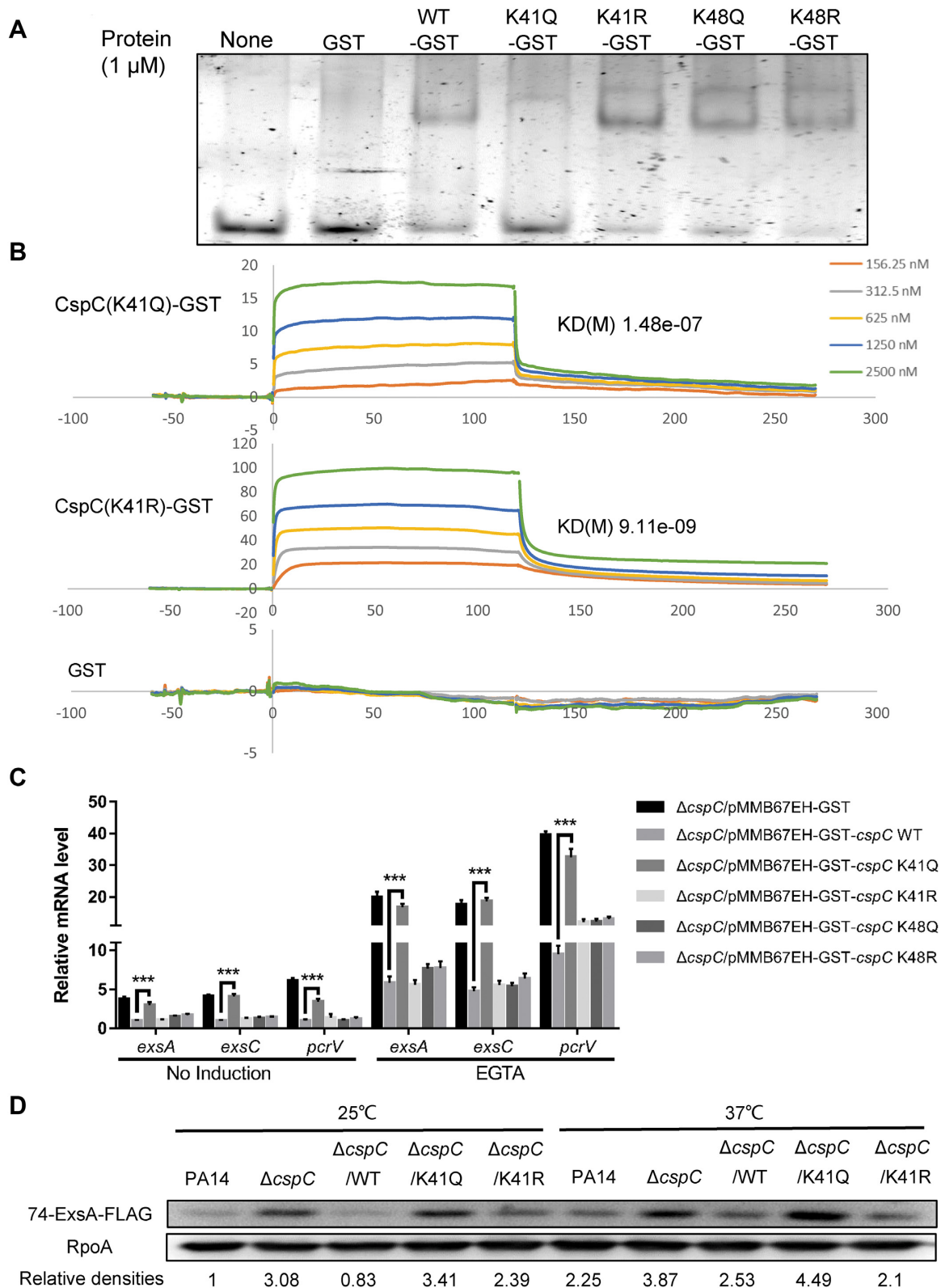


**Figure 5.** The acetylation of CspC influences its function in controlling the translation of *exsA*. (A) Equal amounts of GST, CspC(WT)-GST, CspC(K41Q)-GST, CspC(K41R)-GST, CspC(K48Q)-GST and CspC(K48R)-GST were incubated with the 74 nt ssDNA for 30 min at 16°C. The samples were subjected to electrophoresis in a native gel, followed by staining with SYBR Gold Nucleic Acid Gel Stain. (B) Binding affinities of CspC(K41Q)-GST, CspC(K41R)-GST and GST to the 74 nt ssDNA were determined by an SPR assay. (C) Relative mRNA levels of *exsA*, *exsC* and *pcrV*. Total RNA of indicated strains was isolated from bacteria grown in LB containing 150  $\mu$ g/ml carbenicillin with or without 5 mM EGTA at 37°C. The mRNA levels were determined by qRT-PCR. Data represent the mean of three independent experiments and error bars indicate standard deviation. \*\*\*,  $P < 0.001$  by Student's *t*-test. (D) Indicated strains carrying the  $P_{tac}$ -74-*exsA*-FLAG were grown to an OD<sub>600</sub> of 1.0 in LB containing 150  $\mu$ g/ml carbenicillin at 25°C or 37°C. The ExsA-FLAG levels were determined by western blot.

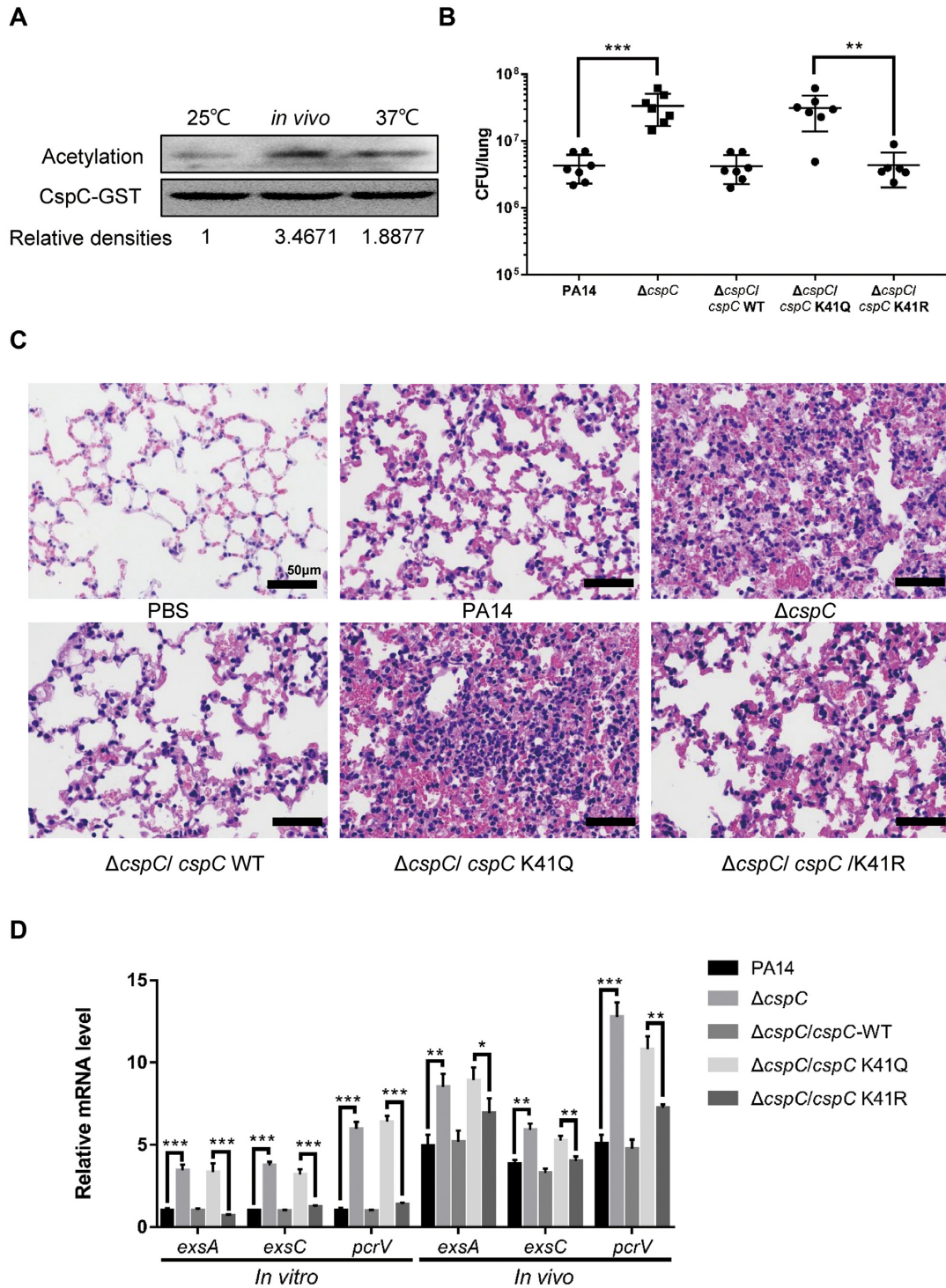


**Figure 6.** Mutations of the K41 residue affected the function of CspC *in vivo*. (A) The  $\Delta$ *pscC* mutant carrying the *cspC-gst* was grown in LB containing 150  $\mu$ g/ml carbenicillin to an OD<sub>600</sub> of 1.0 at 25°C or 37°C. Mice were inoculated intranasally with  $1 \times 10^9$  CFU bacteria. At 4 hpi, bacteria from BALF were collected, followed by chromatography purification. Acetylation and the total amounts of the purified CspC-GST were determined by western blot. (B) Mice were inoculated intranasally with  $4 \times 10^6$  CFU bacteria of the indicated strains. At 12 hpi, the mice were sacrificed and lungs were isolated and homogenized. The bacterial loads were determined by serial dilution and plating. The central bar indicates the mean, and the error bar indicates standard error. \*\* $P < 0.01$ , \*\*\* $P < 0.001$  by the Mann-Whitney test. (C) Pathology sections of lungs infected with the indicated strains. Mice were infected with  $4 \times 10^6$  CFU of wild-type PA14, the  $\Delta$ *cspC* mutant, the  $\Delta$ *cspC* mutant complemented with wild-type *cspC* or the K41Q, K41R variants. Sterilized PBS was used as a negative control. Lungs from the infected mice were removed, fixed, sectioned and stained with hematoxylin and eosin. Images were taken with a 40  $\times$  objective lens. (D) Relative mRNA levels of T3SS genes and *cspC* before or during lung infection. Mice were infected intranasally with  $1 \times 10^7$  CFU bacteria of the indicated strains. At 6 hpi, bacteria from BALF were collected, followed by RNA isolation. The mRNA levels of *exsA*, *exsC* and *pcrV* were determined by qRT-PCR. Data represent the mean of three independent experiments and error bars indicate standard deviation. \*\*\*,  $P < 0.001$ , \*\*,  $P < 0.01$ , \*,  $P < 0.05$  by Student's *t*-test, ND, not detected.

ondary structure, which interferes with the access of ribosomes. Further studies are required to decipher the molecular mechanism on the CspC-mediated regulation on the *exsA* translation. In addition, the RIP-seq assay was performed under the T3SS non-inducing condition. Under the inducing condition, such as in the presence of EGTA, contact with host cells, additional regulatory targets of CspC might be identified by the RIP-seq assay.

By analyzing the RIP-seq result, we were unable to identify a consensus CspC binding sequence. In other bacteria, no consensus binding sequence of CspA family proteins has been found so far, which might be due to the short target sequence (estimated to be 5–7 nt) (38,56,57).

PTMs have been shown to play vital roles in bacterial metabolism, environmental stress responses and virulence (52,58–62). Previous proteomic studies on the wild-type PA14 grown in a minimal glucose medium identified 320 acetylated proteins, mainly including virulence factors, the DNA-binding protein HU and those involved in carbon metabolism, oxidative stress response and LPS biosynthesis (63–65). Carbon sources have been shown to influence PTM in bacteria (66–69)

In a study utilizing various carbon sources in minimal medium, it was demonstrated that growth with citrate resulted in a high level of acetylated proteins in PA14 (70). In that study, CspC was found to be succinylated but not acetylated (70). However, our current study revealed acetylation but not succinylation of the CspC. We speculated that the discrepancy might be due to growth conditions, as we grew the bacteria in LB.

Here we found that the K41 is acetylated in CspC, which affects its function in the regulation of *exsA*. We believe it is the first report on the functional study on the acetylation of bacterial cold shock proteins. Acetylation of the K41 might neutralize its positive charge, thus reduces the binding affinity between CspC and its target nucleotides. Indeed, there was ~10-fold difference in the binding affinity to the *exsA* 5'-UTR between K41R and K41Q versions of the CspC that mimic unacetylated and acetylated forms, respectively. We further demonstrated a higher percentage of acetylated CspC during lung infection than that grown *in vitro*. Accordingly, we propose that the acetylation of CspC may play an important role in the bacterial response to host *in vivo* environment. The K41Q mutation abolished the CspC function in repressing the *exsA* translation under both *in vitro* and *in vivo* conditions. Although the K41R mutation did not enhance the function of CspC in terms of repressing the translation of *exsA* compared to the wild-type form, it abolished the temperature responsive regulation on the translation of *exsA* (Figure 5D). We suspect that substitution of the amino acid may have affected the protein structure, thus influenced its function.

Acetylation of lysine can be catalyzed by lysine acetyltransferases or occur nonenzymatically, using acetyl phosphate or acetyl-CoA as the donor (59,71,72). Meanwhile, deacetylation is catalyzed by deacetylases (60). Based on genome annotation of the *P. aeruginosa* strain PA14, there are total 91 acetyltransferases and 13 deacetylases ([www.pseudomonas.com](http://www.pseudomonas.com)) (42). However, the acetyltransferase or deacetylase involved in PTM has not been identified in *P. aeruginosa*. Temperature or carbon source shift might affect

the intracellular level of acetyl phosphate or acetyl-CoA as well as the expression level and activities of the acetyltransferase or deacetylase, which influence the global PTM in the cell. Identification of the acetyltransferases and deacetylases as well as the metabolism under different growth conditions will shed light on the regulatory mechanisms of the PTM of CspC and other proteins in response to environmental signals. Our results demonstrated a higher level of CspC acetylation in the bacteria isolated from BALF compared to that grown in LB at 37°C, indicating that the *in vivo* environment, presumably the nutrient compositions, might promote acetylation of the CspC.

Overall, our results demonstrate a role of the CspA family protein CspC in the virulence of *P. aeruginosa* and revealed a novel regulatory mechanism of the T3SS via CspC acetylation. Further studies are warranted for a deeper understanding of the CspC-mediated regulatory pathways in *P. aeruginosa*.

## DATA AVAILABILITY

The datasets generated during the current study are available in the the NCBI Short Read Archive (SRA) repository with an accession number PRJNA690968.

## SUPPLEMENTARY DATA

Supplementary Data are available at NAR Online.

## FUNDING

National Key Research and Development Program of China [2021YFE0101700, 2017YFE0125600]; National Natural Science Foundation of China [82061148018, 31970179, 31970680, 31900115, 31870130]; Tianjin Municipal Science and Technology Commission [19JCYBJC24700]. Funding for open access charge: National Key Research and Development Project of China [2017YFE0125600].

*Conflict of interest statement.* None declared.

## REFERENCES

- Mandin,P. and Johansson,J. (2020) Feeling the heat at the millennium: thermosensors playing with fire. *Mol. Microbiol.*, **113**, 588–592.
- Lam,O., Wheeler,J. and Tang,C.M. (2014) Thermal control of virulence factors in bacteria: a hot topic. *Virulence*, **5**, 852–862.
- Lyczak,J.B., Cannon,C.L. and Pier,G.B. (2002) Lung infections associated with cystic fibrosis. *Clin. Microbiol. Rev.*, **15**, 194–222.
- Gellatly,S.L. and Hancock,R.E. (2013) *Pseudomonas aeruginosa*: new insights into pathogenesis and host defenses. *Pathog. Dis.*, **67**, 159–173.
- Sousa,A.M. and Pereira,M.O. (2014) *Pseudomonas aeruginosa* diversification during infection development in cystic fibrosis lungs—a review. *Pathogens*, **3**, 680–703.
- Wurtzel,O., Yoder-Himes,D.R., Han,K., Dandekar,A.A., Edelleit,S., Greenberg,E.P., Sorek,R. and Lory,S. (2012) The single-nucleotide resolution transcriptome of *Pseudomonas aeruginosa* grown in body temperature. *PLoS Pathog.*, **8**, e1002945.
- Hauser,A.R. and Engel,J.N. (1999) *Pseudomonas aeruginosa* induces type-III-secretion-mediated apoptosis of macrophages and epithelial cells. *Infect. Immun.*, **67**, 5530–5537.
- Schulert,G.S., Feltman,H., Rabin,S.D., Martin,C.G., Battle,S.E., Rello,J. and Hauser,A.R. (2003) Secretion of the toxin ExoU is a marker for highly virulent *Pseudomonas aeruginosa* isolates obtained

- from patients with hospital-acquired pneumonia. *J. Infect. Dis.*, **188**, 1695–1706.
9. Sawa, T. (2014) The molecular mechanism of acute lung injury caused by *Pseudomonas aeruginosa*: from bacterial pathogenesis to host response. *J. Intensive Care*, **2**, 10.
  10. Smith, R.S., Wolfgang, M.C. and Lory, S. (2004) An adenylate cyclase-controlled signaling network regulates *Pseudomonas aeruginosa* virulence in a mouse model of acute pneumonia. *Infect. Immun.*, **72**, 1677–1684.
  11. Hauser, A.R. (2009) The type III secretion system of *Pseudomonas aeruginosa*: infection by injection. *Nat. Rev. Microbiol.*, **7**, 654–665.
  12. Howell, H.A., Logan, L.K. and Hauser, A.R. (2013) Type III secretion of ExoU is critical during early *Pseudomonas aeruginosa* pneumonia. *mBio*, **4**, e00032-00013.
  13. Brutinel, E.D. and Yahr, T.L. (2008) Control of gene expression by type III secretory activity. *Curr. Opin. Microbiol.*, **11**, 128–133.
  14. McCaw, M.L., Lykken, G.L., Singh, P.K. and Yahr, T.L. (2002) ExsD is a negative regulator of the *Pseudomonas aeruginosa* type III secretion regulon. *Mol. Microbiol.*, **46**, 1123–1133.
  15. Dasgupta, N., Lykken, G.L., Wolfgang, M.C. and Yahr, T.L. (2004) A novel anti-anti-activator mechanism regulates expression of the *Pseudomonas aeruginosa* type III secretion system. *Mol. Microbiol.*, **53**, 297–308.
  16. Rietsch, A., Vallet-Gely, I., Dove, S.L. and Mekalanos, J.J. (2005) ExsE, a secreted regulator of type III secretion genes in *Pseudomonas aeruginosa*. *Proc. Natl Acad. Sci. U.S.A.*, **102**, 8006–8011.
  17. Urbanowski, M.L., Lykken, G.L. and Yahr, T.L. (2005) A secreted regulatory protein couples transcription to the secretory activity of the *Pseudomonas aeruginosa* type III secretion system. *Proc. Natl Acad. Sci. U.S.A.*, **102**, 9930–9935.
  18. Thibault, J., Faudry, E., Ebel, C., Attree, I. and Elsen, S. (2009) Anti-activator ExsD forms a 1:1 complex with ExsA to inhibit transcription of type III secretion operons. *J. Biol. Chem.*, **284**, 15762–15770.
  19. Williams McMackin, E.A., Djajagne, L., Corley, J.M. and Yahr, T.L. (2019) Fitting pieces into the puzzle of *Pseudomonas aeruginosa* type III secretion system gene expression. *J. Bacteriol.*, **201**, e00209-19.
  20. Wolfgang, M.C., Lee, V.T., Gilmore, M.E. and Lory, S. (2003) Coordinate regulation of bacterial virulence genes by a novel adenylate cyclase-dependent signaling pathway. *Dev. Cell*, **4**, 253–263.
  21. Fuchs, E.L., Brutinel, E.D., Klem, E.R., Fehr, A.R., Yahr, T.L. and Wolfgang, M.C. (2010) *In vitro* and *in vivo* characterization of the *Pseudomonas aeruginosa* cyclic AMP (cAMP) phosphodiesterase CpdA, required for cAMP homeostasis and virulence factor regulation. *J. Bacteriol.*, **192**, 2779–2790.
  22. Almlad, H., Harrison, J.J., Rybke, M., Groizeleau, J., Givskov, M., Parsek, M.R. and Tolker-Nielsen, T. (2015) The cyclic AMP-Vfr signaling pathway in *Pseudomonas aeruginosa* is inhibited by cyclic Di-GMP. *J. Bacteriol.*, **197**, 2190–2200.
  23. Marsden, A.E., Intile, P.J., Schulmeyer, K.H., Simmons-Patterson, E.R., Urbanowski, M.L., Wolfgang, M.C. and Yahr, T.L. (2016) Vfr directly activates exsA transcription to regulate expression of the *Pseudomonas aeruginosa* type III secretion system. *J. Bacteriol.*, **198**, 1442–1450.
  24. Kim, J., Ahn, K., Min, S., Jia, J., Ha, U., Wu, D. and Jin, S. (2005) Factors triggering type III secretion in *Pseudomonas aeruginosa*. *Microbiology (Reading)*, **151**, 3575–3587.
  25. Hayes, C.S., Aoki, S.K. and Low, D.A. (2010) Bacterial contact-dependent delivery systems. *Annu. Rev. Genet.*, **44**, 71–90.
  26. Phadtare, S. (2004) Recent developments in bacterial cold-shock response. *Curr. Issues Mol. Biol.*, **6**, 125–136.
  27. Horn, G., Hofweber, R., Kremer, W. and Kalbitzer, H.R. (2007) Structure and function of bacterial cold shock proteins. *Cell. Mol. Life Sci.*, **64**, 1457–1470.
  28. Caruso, I.P., Panwalkar, V., Coronado, M.A., Dingley, A.J., Cornelio, M.L., Willbold, D., Arni, R.K. and Eberle, R.J. (2018) Structure and interaction of *Corynebacterium pseudotuberculosis* cold shock protein A with Y-box single-stranded DNA fragment. *FEBS J.*, **285**, 372–390.
  29. Keto-Timonen, R., Hietala, N., Palonen, E., Hakakorpi, A., Lindstrom, M. and Korkeala, H. (2016) Cold shock proteins: a minireview with special emphasis on Csp-family of enteropathogenic yersinia. *Front. Microbiol.*, **7**, 1151.
  30. Wang, Z., Wang, S. and Wu, Q. (2014) Cold shock protein A plays an important role in the stress adaptation and virulence of *Brucella melitensis*. *FEMS Microbiol. Lett.*, **354**, 27–36.
  31. Yu, T., Keto-Timonen, R., Jiang, X., Virtanen, J.P. and Korkeala, H. (2019) Insights into the phylogeny and evolution of cold shock proteins: from enteropathogenic yersinia and *Escherichia coli* to eubacteria. *Int. J. Mol. Sci.*, **20**, 4059.
  32. Fang, L., Jiang, W., Bae, W. and Inouye, M. (1997) Promoter-independent cold-shock induction of cspA and its derepression at 37 degrees C by mRNA stabilization. *Mol. Microbiol.*, **23**, 355–364.
  33. Phadtare, S. and Severinov, K. (2005) Nucleic acid melting by *Escherichia coli* CspE. *Nucleic Acids Res.*, **33**, 5583–5590.
  34. Phadtare, S. and Severinov, K. (2010) RNA remodeling and gene regulation by cold shock proteins. *RNA Biol.*, **7**, 788–795.
  35. Duval, B.D., Mathew, A., Satola, S.W. and Shafer, W.M. (2010) Altered growth, pigmentation and antimicrobial susceptibility properties of *Staphylococcus aureus* due to loss of the major cold shock gene cspB. *Antimicrob. Agents Chemother.*, **54**, 2283–2290.
  36. Santos, J.S., da Silva, C.A., Balhasteros, H., Lourenco, R.F. and Marques, M.V. (2015) CspC regulates the expression of the glyoxylate cycle genes at stationary phase in caulobacter. *BMC Genomics*, **16**, 638.
  37. Townsley, L., Sison Mangus, M.P., Mehic, S. and Yildiz, F.H. (2016) Response of *Vibrio cholerae* to low-temperature shifts: CspV regulation of type VI secretion, biofilm formation, and association with zooplankton. *Appl. Environ. Microbiol.*, **82**, 4441–4452.
  38. Caballero, C.J., Menendez-Gil, P., Catalan-Moreno, A., Vergara-Irigaray, M., Garcia, B., Segura, V., Irurzun, N., Villanueva, M., Ruiz de Los Mozos, I., Solano, C. et al. (2018) The regulon of the RNA chaperone CspA and its auto-regulation in *Staphylococcus aureus*. *Nucleic Acids Res.*, **46**, 1345–1361.
  39. Ray, S., Da Costa, R., Thakur, S. and Nandi, D. (2020) *Salmonella Typhimurium* encoded cold shock protein E is essential for motility and biofilm formation. *Microbiology (Reading)*, **166**, 460–473.
  40. Li, K., Yang, G., Debru, A.B., Li, P., Zong, L., Li, P., Xu, T., Wu, W., Jin, S. and Bao, Q. (2017) SuhB regulates the motile-sessile switch in *Pseudomonas aeruginosa* through the Gac/Rsm pathway and c-di-GMP signaling. *Front. Microbiol.*, **8**, 1045.
  41. Xia, B., Li, M., Tian, Z., Chen, G., Liu, C., Xia, Y., Jin, Y., Bai, F., Cheng, Z., Jin, S. et al. (2019) Oligoribonuclease contributes to tolerance to aminoglycoside and beta-lactam antibiotics by regulating KatA in *Pseudomonas aeruginosa*. *Antimicrob. Agents Chemother.*, **63**, e00212-19.
  42. Winsor, G.L., Griffiths, E.J., Lo, R., Dhillon, B.K., Shay, J.A. and Brinkman, F.S. (2016) Enhanced annotations and features for comparing thousands of pseudomonas genomes in the pseudomonas genome database. *Nucleic Acids Res.*, **44**, D646–D653.
  43. Deng, X., Li, M., Pan, X., Zheng, R., Liu, C., Chen, F., Liu, X., Cheng, Z., Jin, S. and Wu, W. (2017) Fis regulates type III secretion system by influencing the transcription of exsA in *Pseudomonas aeruginosa* strain PA14. *Front. Microbiol.*, **8**, 669.
  44. Pan, X., Dong, Y., Fan, Z., Liu, C., Xia, B., Shi, J., Bai, F., Jin, Y., Cheng, Z., Jin, S. et al. (2017) *In vivo* host environment alters *Pseudomonas aeruginosa* susceptibility to aminoglycoside antibiotics. *Front. Cell Infect. Microbiol.*, **7**, 83.
  45. Winsor, G.L., Lam, D.K., Fleming, L., Lo, R., Whiteside, M.D., Yu, N.Y., Hancock, R.E. and Brinkman, F.S. (2011) Pseudomonas genome database: improved comparative analysis and population genomics capability for pseudomonas genomes. *Nucleic Acids Res.*, **39**, D596–D600.
  46. Czapski, T.R. and Trun, N. (2014) Expression of csp genes in *E. coli* K-12 in defined rich and defined minimal media during normal growth, and after cold-shock. *Gene*, **547**, 91–97.
  47. Kumar, S., Stecher, G., Li, M., Nknyaz, C. and Tamura, K. (2018) MEGA X: molecular evolutionary genetics analysis across computing platforms. *Mol. Biol. Evol.*, **35**, 1547–1549.
  48. Yamanaka, K. and Inouye, M. (1997) Growth-phase-dependent expression of cspD, encoding a member of the CspA family in *Escherichia coli*. *J. Bacteriol.*, **179**, 5126–5130.
  49. Giuliodori, A.M., Fabbretti, A. and Gualerzi, C. (2019) Cold-responsive regions of paradigm cold-shock and non-cold-shock mRNAs responsible for cold shock translational bias. *Int. J. Mol. Sci.*, **20**, 457.

50. Phadtare, S. and Inoué, M. (1999) Sequence-selective interactions with RNA by CspB, CspC and CspE, members of the CspA family of *Escherichia coli*. *Mol. Microbiol.*, **33**, 1004–1014.
51. Intile, P.J., Balzer, G.J., Wolfgang, M.C. and Yahr, T.L. (2015) The RNA helicase DeaD stimulates ExsA translation to promote expression of the *Pseudomonas aeruginosa* type III secretion system. *J. Bacteriol.*, **197**, 2664–2674.
52. Christensen, D.G., Baumgartner, J.T., Xie, X., Jew, K.M., Basisty, N., Schilling, B., Kuhn, M.L. and Wolfe, A.J. (2019) Mechanisms, detection, and relevance of protein acetylation in prokaryotes. *mBio*, **10**, e02708-18.
53. Diaz, M.R., King, J.M. and Yahr, T.L. (2011) Intrinsic and extrinsic regulation of type III secretion gene expression in *Pseudomonas aeruginosa*. *Front. Microbiol.*, **2**, 89.
54. Galle, M., Carpentier, I. and Beyaert, R. (2012) Structure and function of the type III secretion system of *Pseudomonas aeruginosa*. *Curr. Protein Pept. Sci.*, **13**, 831–842.
55. Michaux, C., Holmqvist, E., Vasicek, E., Sharan, M., Barquist, L., Westermann, A.J., Gunn, J.S. and Vogel, J. (2017) RNA target profiles direct the discovery of virulence functions for the cold-shock proteins CspC and CspE. *Proc. Natl Acad. Sci. U.S.A.*, **114**, 6824–6829.
56. Sachs, R., Max, K.E., Heinemann, U. and Balbach, J. (2012) RNA single strands bind to a conserved surface of the major cold shock protein in crystals and solution. *RNA*, **18**, 65–76.
57. Pop, C., Rouskin, S., Ingolia, N.T., Han, L., Phizicky, E.M., Weissman, J.S. and Koller, D. (2014) Causal signals between codon bias, mRNA structure, and the efficiency of translation and elongation. *Mol. Syst. Biol.*, **10**, 770.
58. Hentchel, K.L. and Escalante-Semerena, J.C. (2015) Acylation of biomolecules in prokaryotes: a widespread strategy for the control of biological function and metabolic stress. *Microbiol. Mol. Biol. Rev.*, **79**, 321–346.
59. Ren, J., Sang, Y., Lu, J. and Yao, Y.F. (2017) Protein acetylation and its role in bacterial virulence. *Trends Microbiol.*, **25**, 768–779.
60. Macek, B., Forchhammer, K., Hardouin, J., Weber-Ban, E., Grangeasse, C. and Mijakovic, I. (2019) Protein post-translational modifications in bacteria. *Nat. Rev. Microbiol.*, **17**, 651–664.
61. Chambers, K.A. and Scheck, R.A. (2020) Bacterial virulence mediated by orthogonal post-translational modification. *Nat. Chem. Biol.*, **16**, 1043–1051.
62. Koo, H., Park, S., Kwak, M.K. and Lee, J.S. (2020) Regulation of gene expression by protein lysine acetylation in *Salmonella*. *J. Microbiol.*, **58**, 979–987.
63. Ouidir, T., Cosette, P., Jouenne, T. and Hardouin, J. (2015) Proteomic profiling of lysine acetylation in *Pseudomonas aeruginosa* reveals the diversity of acetylated proteins. *Proteomics*, **15**, 2152–2157.
64. Schilling, B., Christensen, D., Davis, R., Sahu, A.K., Hu, L.L., Walker-Peddakotla, A., Sorensen, D.J., Zemaitaitis, B., Gibson, B.W. and Wolfe, A.J. (2015) Protein acetylation dynamics in response to carbon overflow in *Escherichia coli*. *Mol. Microbiol.*, **98**, 847–863.
65. Gaviard, C., Cosette, P., Jouenne, T. and Hardouin, J. (2019) LasB and CbpD virulence factors of *Pseudomonas aeruginosa* carry multiple post-translational modifications on their lysine residues. *J. Proteome Res.*, **18**, 923–933.
66. Zhang, Z., Tan, M., Xie, Z., Dai, L., Chen, Y. and Zhao, Y. (2011) Identification of lysine succinylation as a new post-translational modification. *Nat. Chem. Biol.*, **7**, 58–63.
67. Colak, G., Xie, Z., Zhu, A.Y., Dai, L., Lu, Z., Zhang, Y., Wan, X., Chen, Y., Cha, Y.H., Lin, H. *et al.* (2013) Identification of lysine succinylation substrates and the succinylation regulatory enzyme CobB in *Escherichia coli*. *Mol. Cell. Proteomics*, **12**, 3509–3520.
68. Kosono, S., Tamura, M., Suzuki, S., Kawamura, Y., Yoshida, A., Nishiyama, M. and Yoshida, M. (2015) Changes in the acetylome and succinylome of *Bacillus subtilis* in response to carbon source. *PLoS One*, **10**, e0131169.
69. Mizuno, Y., Nagano-Shoji, M., Kubo, S., Kawamura, Y., Yoshida, A., Kawasaki, H., Nishiyama, M., Yoshida, M. and Kosono, S. (2016) Altered acetylation and succinylation profiles in *Corynebacterium glutamicum* in response to conditions inducing glutamate overproduction. *Microbiologyopen*, **5**, 152–173.
70. Gaviard, C., Broutin, I., Cosette, P., De, E., Jouenne, T. and Hardouin, J. (2018) Lysine succinylation and acetylation in *Pseudomonas aeruginosa*. *J. Proteome Res.*, **17**, 2449–2459.
71. Wolfe, A.J. (2016) Bacterial protein acetylation: new discoveries unanswered questions. *Curr. Genet.*, **62**, 335–341.
72. Liu, W., Tan, Y., Cao, S., Zhao, H., Fang, H., Yang, X., Wang, T., Zhou, Y., Yan, Y., Han, Y. *et al.* (2018) Protein acetylation mediated by YfiQ and CobB is involved in the virulence and stress response of *Yersinia pestis*. *Infect. Immun.*, **86**, e00224-18.